Role of helium in the sliding and mechanical properties of a vanadium grain boundary: A first-principles study*

Zhou Hong-Bo(周洪波)†, Jin Shuo(金 硕), Zhang Ying(张 颖), Shu Xiao-Lin(舒小林), and Niu Liang-Liang(牛亮亮)

Department of Physics, Beihang University, Beijing 100191, *China*

(Received 23 July 2013; revised manuscript received 10 January 2014; published online 18 March 2014)

The effects of helium (He) on the sliding and mechanical properties of a vanadium (V) Σ5(310)/[001] grain boundary (GB) have been investigated using a first-principles method. It has been found that He was energetically favorable sitting at the GB region with a segregation energy of −0.27 eV, which was attributed to the special atomic configurations and charge density distributions of the GB. The maximal sliding energy barrier of the He-doped GB was calculated to be 1.73 J/m^2, ∼ 35% larger than that of the clean GB. This suggested that the presence of He would hinder the V GB mobility. Based on the thermodynamic criterion, the total energy calculations indicated that the embrittlement of V GB would be enhanced by He segregation.

Keywords: helium, vanadium grain boundary, sliding properties, mechanical properties

PACS: 61.80.Az, 71.20.Be, 61.72.Mm, 62.20.F− **DOI:** 10.1088/1674-1056/23/5/056104

1. Introduction

Nowadays, the energy shortage drives us to spend great efforts to develop nuclear fusion techniques, which will be of practical use in the foreseeable future. Fusion energy is being developed universally via the international thermonuclear experimental reactor (ITER) project.[1] The final application of nuclear fusion energy is mainly dependent on the development of materials in the thermonuclear fusion device "Tokamak", in which the choice of structural material is one of the key issues. Vanadium (V) and V alloys are regarded as the most promising candidates for the structural materials because of their excellent mechanical properties, high thermal conductivity, good resistance to irradiation-induced swelling and damage as well as low activation properties.[2–6] However, as the structural material of fusion reactors, V will be irradiated by high energy neutrons, which leads to large amounts of helium (He) produced from (n, α) transmutation reactions in V.[7,8] Although the solubility of He in metals is extremely low, it can lead to significant changes in microstructure and mechanical properties.[9,10] Consequently, understanding the role of He in the V system is a critical issue in the development of structural materials in fusion reactors.

Helium is characterized by its closed-shell electronic structure, and prefers to keep such structure when it goes into different environments. Any interaction with other elements which breaks such a structure can elevate the system energy. Thus, He prefers to occupy the site with a large effective volume in metals. Generally, defects in materials, such as grain boundaries (GBs), dislocations and vacancies, are considered to be the main regions for He dissolution and accumulation in V. The role of GBs gets much more attention among them. GB is one of the main defects in materials, acting as a transition region between two adjacent crystal lattices, and thus the chemical composition and crystallographic structure of GBs are distinct from those of the bulk crystal.[11] Some elements will segregate to GBs due to the different chemical composition between GBs and the surrounding bulk.[12] In previous experimental studies,[13–19] GBs have been demonstrated to be one of the most propitious sites for He accumulation in V. Most of the He produced by transmutation would diffuse further in the material, which could eventually find trapping sites and accumulate in GBs.[19] He bubble nucleation at GBs has been observed in V by means of transmission electron microscopy.[13] The mechanical properties of the GB will decrease with the increase of He concentration, and intergranular fracture will occur over a critical He concentration, resulting in a great loss in ductility.[15,18] At high temperature, the intergranular brittle fracture can be realized in V alloys due to the accumulation of He at GBs during the mechanical tests.[13,16]

The sliding of a GB is considered to be one of the principal mechanisms of plastic deformation for polycrystalline materials at high temperatures (above $0.4T_{\rm m}$, where $T_{\rm m}$ is the melting point),[19] which can be described as the relative displacement of the two constituent grains in the direction parallel to the boundary interface. Under irradiation, materials will be driven far from equilibrium.[20] The interaction between irradiation defects and materials should be better understood at a microscopic level in order to investigate how the materials change under irradiation. The pure GB sliding mechanism and the effect of irradiation defects (such as He) on GB are very important for developing models of mechanical behavior in metals under irradiation.[21] However, so far little work focuses on this aspect in V and V alloys. In this paper, we inves-

*Project supported by the National Magnetic Confinement Fusion Program of China (Grant No. 2013GB109002).

†Corresponding author. E-mail: hbzhou@buaa.edu.cn

© 2014 Chinese Physical Society and IOP Publishing Ltd

tigate the effects of He on the sliding and mechanical properties of a Σ5 (310)/[001] V GB using a first-principles method. The choice of this GB is because the Σ5(310)/[001] GB has been experimentally proved to be one of the stable GBs in the bcc metals. Further, it has been widely considered as a representative of GBs to investigate the properties of GB in the bcc metals, such as Fe,[22–24] Mo,[25–27] Nb.[26,28] V is also in the bcc crystal structure, thus the Σ5(310)/[001] GB is chosen as a representative GB in this work. Because irradiation under a fusion environment will produce a large amount of He, this will help us to understand how the irradiation affects the mechanical properties of V from the He point of view.

2. Computational method

We employ a first-principles method based on density functional theory (DFT) with generalized gradient approximation (GGA) according to Perdew and Wang[29] using the vienna *ab-initio* simulation package (VASP).[30–32] The interaction between ions and electrons is described by the projector augmented wave (PAW) potential based on GGA. The energy cutoff for the plane wave basis is chosen to be 350 eV. We model the 36.9° [100]{013}Σ = 5 symmetrical tilt GB in V using a supercell with 68 atoms. Since we have used a periodic boundary condition, we separate the neighboring slabs in the [310] direction by a vacuum region of about 10 Å (1 Å = 10^{-10} m) to minimize the interaction between slabs. The calculated equilibrium lattice constant is 2.98 Å for the bcc V, in good agreement with the corresponding experimental value of 3.03 Å.[33] The supercell sizes are 24.83 Å × 9.57 Å × 5.97Å in the [310], [1$\bar{3}$0], and [001] directions, respectively. For summation over the Brillouin zone, the uniform grids of *k*-points are 1 × 2 × 3 according to the Monkhorst–Pack scheme with relaxation of the atomic positions of the supercell.[34] The energy relaxation iterates until the forces acting on all the atoms are less than 10^{-3} eV/Å.

3. Results and discussion

3.1. Dissolution of single He atom in V GB

In the previous studies,[35,36] it has been demonstrated that a single He is energetically favorable sitting at the tetrahedral interstitial site (TIS) in the bulk V. However, the dissolution behavior of He in V GB is still unclear. Here, in order to find the most favourable site of a single He atom in the V GB, we examine the solution energies of all potential GB sites for He, including interstitial and substitutional cases. We only consider He in the II atom layer, because the sites that He occupies are symmetrically equivalent for the I and II layers, and the I and II layers are totally the same as the periodical III and IV layers. As shown in Fig. 1, the He atom has been assigned to six different interstitial sites (I1–I6) and five different substitutional sites (S1–S5) on the II layer in the V GB. When He occupies an interstitial site, the solution energy of He ($E^{\rm sol}_{\rm GB,int}$) is expressed by

$$E^{\rm sol}_{\rm GB,int} = E^{\rm T}_{\rm GB,He} - E^{\rm T}_{\rm GB} - E_{\rm He}, \quad (1)$$

where $E^{\rm T}_{\rm GB,He}$ and $E^{\rm T}_{\rm GB}$ are the total energies of the V GB supercell with and without He, respectively, and $E_{\rm He}$ is the energy of an isolated He atom. When the He atom replaces a V atom, the solution energy of He ($E^{\rm sol}_{\rm GB,sub}$) can be obtained by

$$E^{\rm sol}_{\rm GB,sub} = E^{\rm T}_{\rm GB,Vacancy,He} - E^{\rm T}_{\rm GB} + E_{\rm V} - E_{\rm He}, \quad (2)$$

where $E^{\rm T}_{\rm GB,Vacancy,He}$ is the total energy of the V GB supercell with a single vacancy and one interstitial He atom, and $E_{\rm V}$ is the energy of a V atom in the V bulk.

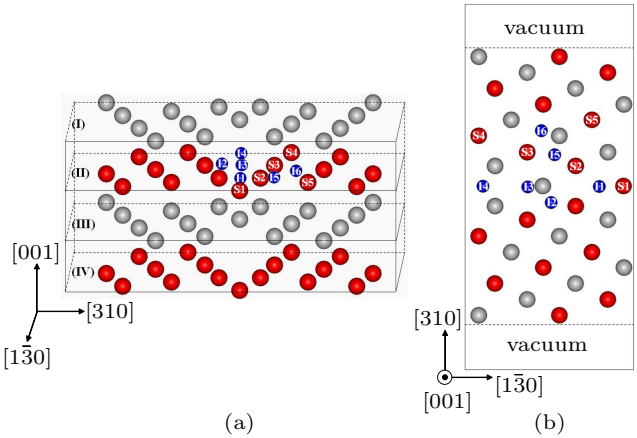


Fig. 1. (color online) (a) The supercell of a Σ5 (310)/[001] V grain boundary, (b) top view of the supercell. The red (darker) and gray (lighter) spheres correspond to the different layers in the supercell. The smaller blue spheres (numbers of I1–I6) represent the six different interstitial sites in the II atom layer. Numbers S1–S5 represent the five different substitutional sites of the He substitution for V.

Figure 2 shows the solution energies as a function of different He occupation sites. In the interstitial cases, it can be found that I3 is the most energetically stable interstitial site with a solution energy of 2.71 eV shown in Fig. 2(a). Since He has a closed shell electronic structure forming very weak chemical bonding with the host metal atoms, the stability of He in metals can be well understood by its "effective volume". The size of He effective volume in metals mainly depends on the distance between He and its surrounding metal atoms, especially the distance between He and its first nearest neighboring (1NN) metal atom. For the I3 case, the distance between He and its 1NN V atom is about 1.94 Å, which is longer than those of He at other sites in the V GB. This leads to that the effective volume of He at the I3 site is largest among all cases, and thus I3 is the most stable interstitial site for He in V GB. However, this is not applicable to the substitutional case. Although the effective volume of He at the substitutional site is larger in comparison with the interstitial cases, the solution energy of the substitutional case is larger than that of the interstitial cases, as illustrated in Fig. 2. This can be attributed to the fact that a V atom will be removed from the V GB when a He atom occupies a substitutional site. Thus, the vacancy formation energy plays a key role in the substitutional cases.

Figure 2(b) shows that the solution energy of S2 is much lower than that of other substitutional sites, which is due to the fact that the V (S2) atom is the easiest to remove from the V GB (lower vacancy formation energy). Further, it can be found that the solution energy of S2 is much larger than that of the I3 case. Therefore, the I3 is the most stable site for He among all cases.

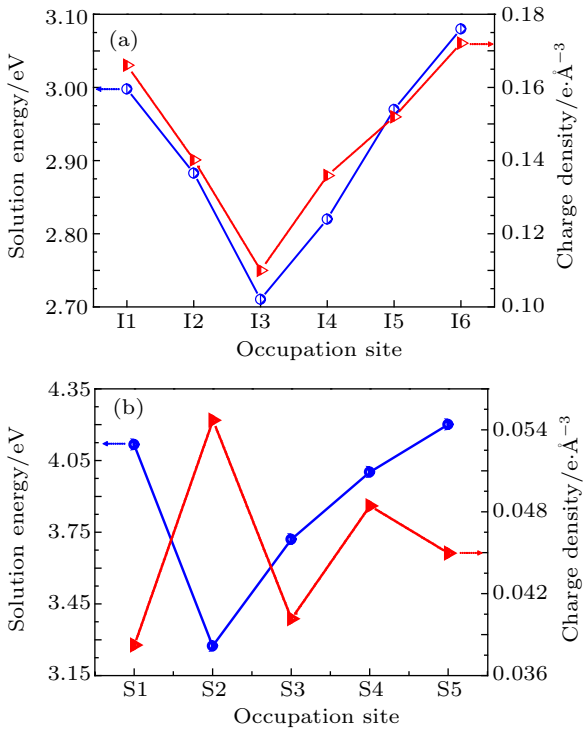


Fig. 2. (color online) The solution energies and charge densities as functions of different He occupation sites: (a) interstitial cases; (b) substitutional cases. The lines are only to guide the eyes.

Physically, the He solution energy in a metal can also be understood approximately in terms of the He solution energy in a homogeneous electron gas.[37] The He solution energy decreases monotonically with the decrease of the electron density until reaching the minimum at the electron density of $n_0 = 0$ electron/Å^3 (e/Å^3), which is the optimal density for He in the homogeneous electron gas model.[37] Since the charge density everywhere in the V GB (as well as in most metals) is much higher than n_0, He generally has the lowest solution energy where the charge density is the lowest. For the V GB, the charge density for the interstitial sites of He after the structure optimization is illustrated in Fig. 2. The solution energy sequence for the optimal interstitial sites of He is I3 < I4 < I2 < I5 < I1 < I6. Such a sequence is consistent with charge density results, that is, the lower the charge density, the lower the solution energy. The most stable interstitial site (I3) corresponds to the lowest charge density. On the other hand, since the solution energy for the substitutional case depends on the vacancy formation energy, the charge density for the substitutional cases does not directly correspond to the solution energies. In the substitutional case, the lowest solution energy occurs at the S2 site, because the vacancy formation energy for the S2 site is much lower than that for the other cases.

In order to show energetically whether He has a tendency to move into the V GB, we calculate the segregation energy of He in the V GB. It can be calculated by

$$E^{\mathrm{seg}} = (E^{\mathrm{T}}_{\mathrm{GB,He}} - E^{\mathrm{T}}_{\mathrm{GB}}) - (E^{\mathrm{T}}_{\mathrm{bulk,He}} - E^{\mathrm{T}}_{\mathrm{bulk}}), \tag{3}$$

where $E^{\mathrm{T}}_{\mathrm{GB,He}}$ and $E^{\mathrm{T}}_{\mathrm{GB}}$ are the total energies of the V GB system with and without He, and $E^{\mathrm{T}}_{\mathrm{bulk,He}}$ and $E^{\mathrm{T}}_{\mathrm{bulk}}$ are the total energies of the V bulk system with and without He. The definition of the segregation energy in the present calculation is essentially the same as that in the previous studies.[38,39] In order to eliminate the effect of GB on He solution energy in the bulk V, we used a bcc bulk V system to determine $E^{\mathrm{T}}_{\mathrm{bulk,He}}$ and $E^{\mathrm{T}}_{\mathrm{bulk}}$. The size of the bulk V system is approximately the same as the corresponding GB system. The lower the segregation energy, the easier the He can move toward the GB. Considering the interstitial case at I3 with the lowest solution energy of 2.71 eV for the V GB and the tetrahedral interstitial case with the lowest solution energy of 2.98 eV for the bulk V according to the present calculations, the segregation energy of He in the V GB is calculated to be −0.27 eV. Thus, He prefers to stay in the V GB instead of in the bulk V. This can be attributed to the fact that the V GB can provide the larger effective volume and lower charge density site for He in comparison with the bulk V.

3.2. Sliding of a clean V GB

It has been demonstrated that the interfacial bonds are very weak in the GB, thus the sliding and fracture of GB occurs more easily along the GB plane.[40–43] The strength of interfacial bonds can be characterized by the cohesive energy of interfacial planes, i.e., the lower the cohesive energy, the weaker the interfacial bond. In order to choose a reasonable sliding plane for the V GB, we have calculated the cohesive energy of interfacial planes between different layers. The cohesive energy of the interfacial plane between the A layer and the B layer is defined as

$$E^{\mathrm{COH}}_{\mathrm{A-B}} = \frac{E^{\mathrm{T}}_{\mathrm{A-Vacuum-B,GB}} - E^{\mathrm{T}}_{\mathrm{GB}}}{S}, \tag{4}$$

where A and B represent two nearest neighboring layers in the V GB, $E^{\mathrm{T}}_{\mathrm{A-Vacuum-B,GB}}$ is the total energy of the V GB system when A and B are separated by a vacuum region of about 10 Å in the [310] direction, and S is the area of the cross section of the supercell. It is found the cohesive energy of the interfacial plane between the first layer of the top (or bottom) grain and the central layer is lowest with 2.11 J/m^{-2}. We thus choose this plane as the sliding plane. The GB sliding is simulated quasistatically, namely the top grain is rigidly shifted over the bottom by a series of small specified distances along

the interface. The sliding distance of the parallel shift is applied to the atoms of the top grain, and then all atoms of the GB are fixed in the sliding direction and freely relaxed in any directions normal to the sliding direction. The starting atomic configuration for each anneal is taken from the previous one. The sliding distance is defined by the percentage of $a_{\rm csl}$, where $a_{\rm csl}$ is the lattice parameter of the coincident site lattice (CSL) cell along the sliding direction. Clearly sliding by $a_{\rm csl}$ will bring the grain boundary back to its original configuration due to the imposed periodic boundary conditions. For each rigid shift, atomic relaxation is performed to locate the closest local energy minimum configuration. The GB sliding energy barrier ($E_{\rm GB}^{\rm SEB}$) is defined as

$$E_{\rm GB}^{\rm SEB} = \frac{E_{\varepsilon,{\rm GB}}^{\rm T} - E_{0,{\rm GB}}^{\rm T}}{S}, \tag{5}$$

where $E_{\varepsilon,{\rm NV,GB}}^{\rm T}$ and $E_{0,{\rm NV,GB}}^{\rm T}$ are the total energies of the V GB supercell with and without GB sliding, and ε is the sliding distance expressed as a percentage of the lattice parameter, $a_{\rm csl}$, of the CLS cell along the $[1\bar{3}0]$ direction.

Figure 3 shows the GB sliding energy barrier as a function of the GB sliding displacement along the $[1\bar{3}0]$ direction. It can be observed that for the clean GB, there are two local maximal GB sliding energy barriers, which occur at the displacement distance of 20% and 70% $a_{\rm csl}$, respectively. The maximal GB sliding energy barrier in the sliding period is ~ 1.28 J/m^2 at the displacement distance of 70% $a_{\rm csl}$. Interestingly, there is one GB sliding energy barrier valley at 42% $a_{\rm csl}$, as illustrated in Fig. 3. At this point, the GB sliding energy barrier is only 0.04 J/m^2, which is 97% lower than the maximal energy barrier. Therefore, the GB sliding process along the $[1\bar{3}0]$ direction can be divided into two regions 0%–42% $a_{\rm csl}$ and 42%–100% $a_{\rm csl}$.

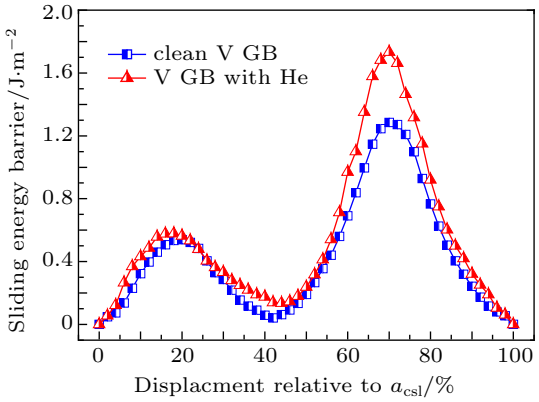


Fig. 3. (color online) The sliding energy barrier of GB without and with He as a function of sliding distance expressed as a percentage of the lattice parameter, $a_{\rm csl}$, of the CLS cell along the $[1\bar{3}0]$ direction. The lines are just a guide for the eyes.

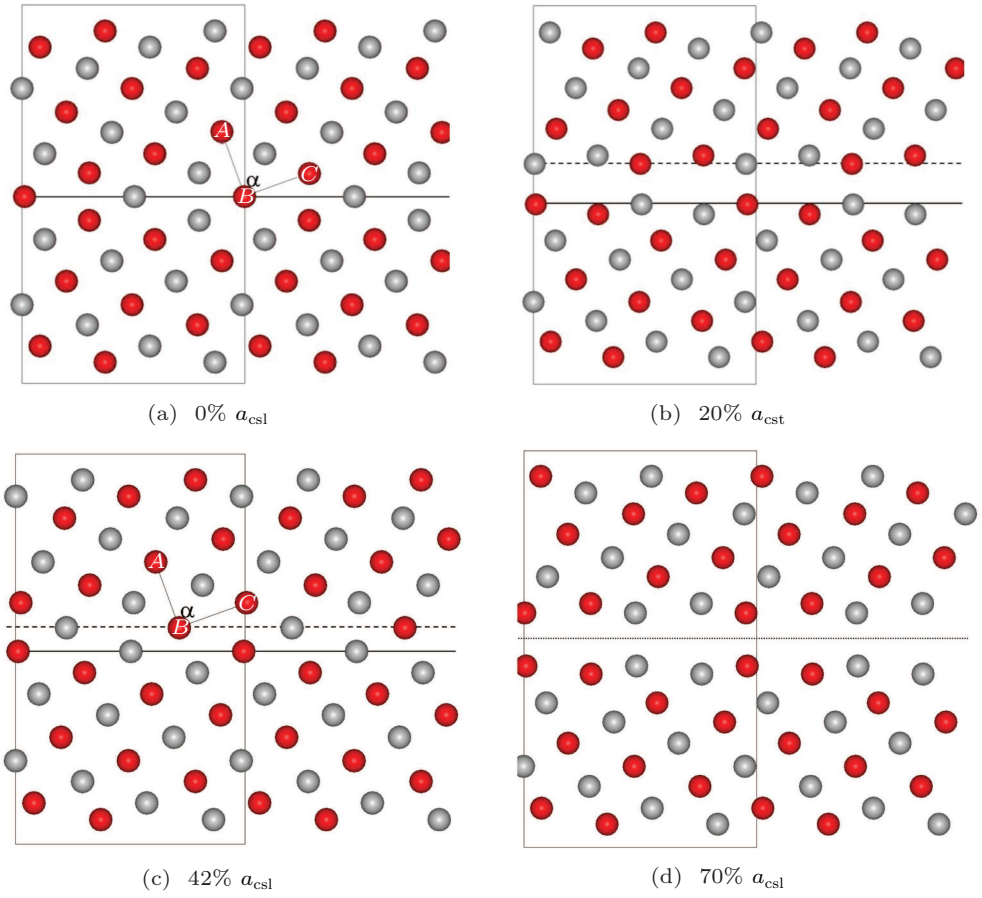


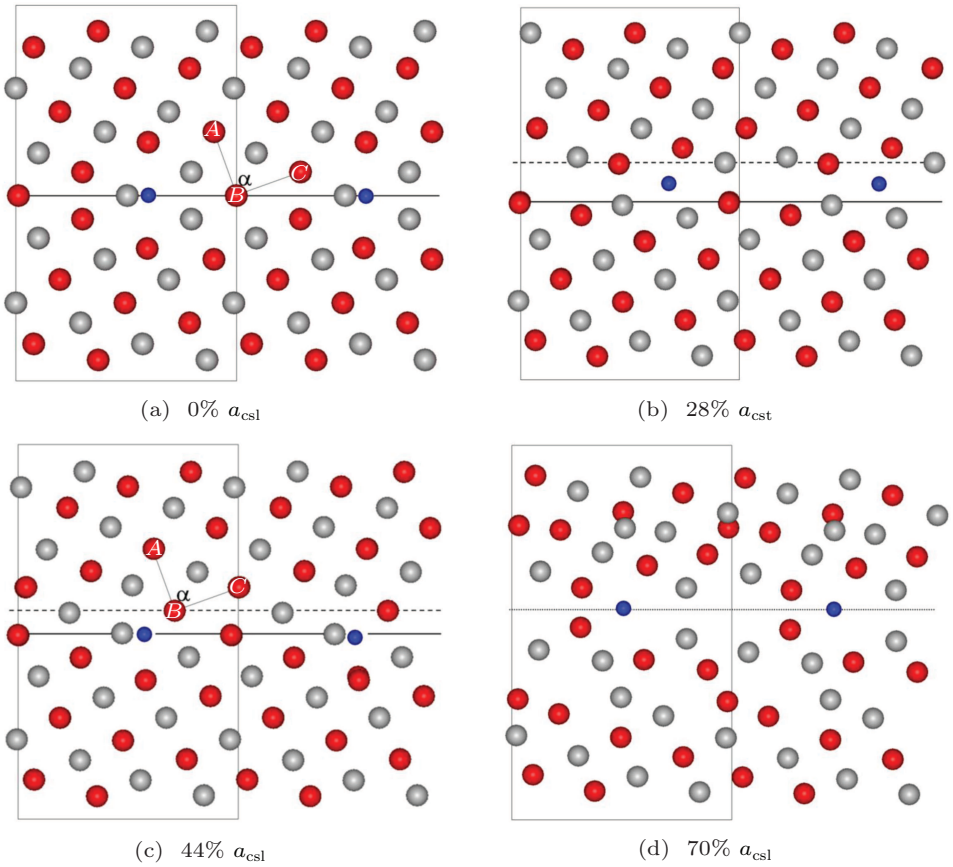
Fig. 4. (color online) Evolution of the atomic structure of the clean GB during the sliding process. The snapshots of the GB structures correspond to the special points (0% (a), 20% (b), 42% (c), and 70% (d) $a_{\rm csl}$) on the GB sliding energy barrier for the clean GB.

We further investigate the atomic configurations and electronic properties associated with the representational special points (0%, 20%, 42%, and 70% a_{csl}), in order to explore the origin of variation of the GB sliding energy barrier. Figure 4 shows the relaxed atomic configurations of these special points. The angle α ($\angle ABC$) of the structural unit in the initial atomic structure of the clean V GB before sliding is very close to that in the bulk V with 90°, as shown in Fig. 4(a). The grain interface is indicated by a solid line. By examining the various atomic configurations, we find that they are all similar before the point of 20% a_{csl}, and the angle α of all configurations turns out to be obtuse from $\sim 90°$. As illustrated in Fig. 4(b), the GB experiences an abrupt overall structural transformation when the interface starts migrating. The solid and dashed lines are the same in Fig. 4(b). Then, the original grain interface (solid line) disappears, and the new grain interface (dashed line) forms. Thus, a local maximal GB sliding energy barrier occurs at the displacement distance of 20% a_{csl}. As shown in Fig. 4(c), the V GB practically recovers its original symmetric structure after the migration is almost completed. Furthermore, the angle α recovers to a similar right angle based on the new grain interface.

The critical configuration GB has to cross is shown in Fig. 4(d), where the GB experiences the maximal sliding energy barrier along the $[1\bar{3}0]$ direction. There is no boundary plane that can be identified. However, a similar "mirror" plane (dotted line) occurs for the atoms on the (001) and (002) planes. This half-way plane reflects the transition position of the sliding interface. Furthermore, the shortest distance between V atoms is 2.25 Å at the point of 70% a_{csl}, which is much shorter than that of the perfect V bulk by 0.33 Å. These lead to the maximal GB sliding energy barrier for the GB sliding along the $[1\bar{3}0]$ direction. After this point, the GB returns to its initial symmetric configuration, and the atomic configuration of 100% a_{csl} is the same as that of 0% a_{csl}, as shown in Fig. 4(a).

3.3. Sliding of a V GB with He

Figure 5(a) shows the most stable atomic configuration of a V GB with a He atom after the structure optimization. We set this as the initial state for the GB sliding with He. The corresponding sliding energy barrier profile is shown in Fig. 3. The pattern of the energy barrier, similar to that of the clean GB, can still be divided into two regions: 0%–44% and 44%–100% a_{csl}. In the former region, the sliding energy barrier reaches its local maxima (~ 0.59 J/m^2) at the displacement distance of 18% a_{csl}. In the latter region, the local maximal sliding energy barrier of 1.73 J/m^2 occurs at the displacement distance of 70% a_{csl}, which is also the maximal value of the sliding energy barrier during the whole sliding process. It is important to note that the maximal sliding energy barrier of GB with He is 0.45 J/m^2 larger than that of the clean GB. This indicates that the presence of He will hinder the V GB mobility, which is consistent with effects of vacancy on the Al GB.[40]



(a) 0% a_{csl} (b) 28% a_{cst}

(c) 44% a_{csl} (d) 70% a_{csl}

Fig. 5. (color online) Evolution of the atomic structure of the GB with He during the sliding process. The snapshots of the GB structures correspond to the special points (0% (a), 18% (b), 44% (c), and 70% (d) a_{csl}) on the GB sliding energy barrier curve for the GB with He. The smaller blue spheres correspond to the He site in the supercell.

In order to explore the effect of He on the GB sliding, we investigate the atomic configurations associated with the representational special points displayed in Fig. 3, including 0%, 18%, 44%, and 70% a_{csl}. Corresponding to these special points, the relaxed atomic configurations are shown in Figs. 5(a)–5(d). The initial atomic structure for the Σ5 (310)/[001] V GB with a He atom is illustrated in Fig. 5(a). Compared with the clean GB with 0% a_{csl} shown in Fig. 4(a), the presence of He induces a local lattice expansion. By examining the various atomic configurations, we find that they are all similar before the point of 44% a_{csl}. For example, as shown in Fig. 5(b), the original grain interface (solid line) disappears, and the new grain interface (dashed line) forms. At the point of 44% a_{csl}, the V GB practically recovers its original symmetric structure after the migration is almost completed, shown in Fig. 5(c). The angle $\alpha(\angle ABC)$ of the structural unit on the new grain boundary is very close to that in the bulk V with 90°. However, it can be clearly observed that He does not find its most stable site at the new GB in comparison with that in the initial atomic structure [Fig. 5(a)], due to the existing of a diffusion barrier blocking He movement at the GB. This leads to the increase of the GB energy, and thus the sliding energy barrier of the GB with He at 44% a_{csl} is larger than that of the clean GB at 42% a_{csl} by 0.09 J/m^2, as shown in Fig. 3.

The He-doped GB experiences the maximal sliding energy barrier at the displacement distance of 70% a_{csl}. Figure 5(d) shows the atomic configuration of the He-doped GB at this point. It can be found that there is no boundary plane that can be identified. However, a similar "mirror" plane (dotted line) occurs for the atoms on the (001) and (002) planes, which is similar to that of the clean GB at 70% a_{csl} [Fig. 4(d)]. Furthermore, it can be found that there is an observable atomic displacement phenomenon induced by He in comparison with that of the clean GB, which can be attributed to the He–V interaction in the GB. As shown in Fig. 6, we display the calculated binding energy between free He and V as a function of the He–V interatomic distance in a vacuum. It shows a strong repulsive interaction between He and V when their interatomic distance is lower than ∼ 2.0 Å. At the displacement distance of 70% a_{csl}, the distance between He and its nearest neighboring V atoms is 1.79 Å, which is much lower than 2.0 Å. Thus, there is a strong repulsive interaction between He and its neighboring V atoms at this point. The V atoms surrounding He will deviate from normal positions induced by the He–V repulsive interaction in comparison with the He-free case. Further, the energetics of the GB is controlled by the atomic configuration. Thus, the local atomic displacement of the He-doped GB induced by the He–V interaction will lead to the increase of the GB energy, and result in the increase of the GB sliding energy barrier. Consequently, the corresponding maximal sliding energy barrier increases from 1.28 J/m^2 (clean GB) to 1.73 J/m^2 (GB with He). After 70% a_{csl}, the GB returns to its initial symmetric configuration, and the atomic configuration of 100% a_{csl} is the same as that of 0% a_{csl}, as shown in Fig. 5(a).

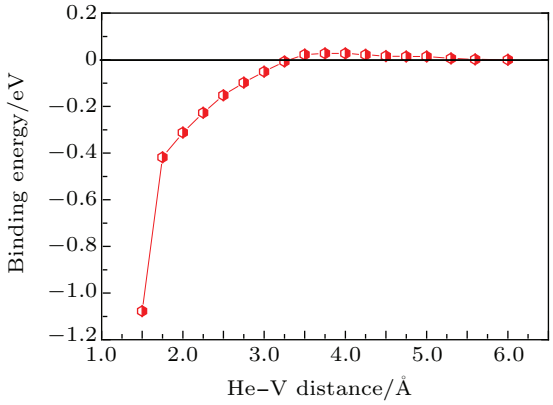


Fig. 6. (color online) The calculated binding energy (eV) of a He–V pair in a vacuum as a function of the He–V spatial separation (Å). Positive values indicate attraction, while negative ones indicate repulsion.

3.4. Mechanical properties affected by He

On an atomic level, brittle versus ductile behavior of a solid material can be described by two competing processes, (i) the opening of a crack and (ii) the emission of dislocations at the crack tip.[44,45] A material is expected to be ductile when the emission of a dislocation is energetically favorable over cleavage at the crack tip.[46] Process (i) is modeled by the cleavage energy (γ_{cl}), which is the energy required per unit area to separate the solid into two semi-infinite halves by creating two surfaces, considered as the lower bound to the actual energy cost measured in a cleavage experiment.[47] Process (ii) is the dislocation emission closely related to the unstable stacking fault energy (γ_{us}), defined as the maximum of the sliding energy barrier (generalized stacking fault energy) by $\gamma_{us} = E^{SEB}_{max}$, represents the energy barrier for dislocation nucleation from a crack tip. Such a method has been successfully applied in investigating the effect of impurities/alloying elements on the mechanical properties of materials with different crystal structures, such as Al,[48] Mg,[49] Mg solid solutions.[50]

The ratio of cleavage energy and unstable stacking fault energy (γ_{cl}/γ_{us}) indicates the capability of crack extension, indicating therefore a brittle or ductile behavior of materials. A high value of γ_{cl}/γ_{us} means the crack is resistant to expansion, while a low value of γ_{cl}/γ_{us} means the crack can expand more easily.[44,51] According to the present calculations, γ_{cl} of the clean V GB is 2.11 J/m^2, but it decreases to 1.78 J/m^2 after the addition of one He atom, suggesting that the strength of the V GB will be weakened due to the He presence. The γ_{us} for the clean V GB is 1.28 J/m^2, and it increases to 1.73 J/m^2

for the He-doped V GB. The corresponding γ_{cl}/γ_{us} ratio of the V GB with He system decreases to 1.03 from the original 1.64 of the clean V GB system. In terms of the Rice criterion,[44,51] we infer that a crack at the Σ5 (310) [001] V GB will expand more easily induced by He segregation, resulting in enhanced GB embrittlement by He. This may also be applicable to other types of V GB.

4. Summary

We perform a first-principles calculation to investigate site preference and its effects of He in a V Σ5(310)/[001] GB. We determine the energetically favorable site of He at the V GB according to the calculated solution energies. It costs less energy for He dissolution at the GB than in the bulk V, which is directly associated with the special atomic configurations and charge density distribution of the GB. The solution energy of He at the most stable site in the V GB is 2.71 eV, ~ 0.27 eV lower than that in the bulk V. It is found that the maximal sliding energy barrier of the V GB with He segregation is 1.73 J/m^2, which is approximately 35% larger than that of the clean V GB (1.28 J/m^2), with the implication that the presence of He will hinder the V GB mobility. Helium is shown to decrease the ratio of cleavage energy and unstable stacking fault energy (γ_{cl}/γ_{us}) by $\sim 37\%$ for the V GB system, suggesting that He makes the crack expand more easily, and thus the presence of He will enhance the embrittlement of V GB.

References

[1] Causey R, Wilson K, Venhaus T and Wampler W R 1999 *J. Nucl. Mater.* **266** 467
[2] Gold R E and Bajaj R 1984 *J. Nucl. Mater.* **122** 759
[3] Smith D L, Chung H M, Matsui H and Rowcliffe A F 1998 *Fusion Eng. Des.* **41** 7
[4] Dyomina E V, Fenici P, Kolotov V P and Zucchetti M 1998 *J. Nucl. Mater.* **258** 1784
[5] Nagasaka T, Muroga T, Fukumoto K C, Watanabe H, Grossbeck M L and Chen J 2006 *Nucl. Fusion* **46** 618
[6] Shyrokov V V, Vasyliv C B and Shyrokov O V 2009 *J. Nucl. Mater.* **394** 114
[7] Steiner D 1974 *Nucl. Fusion* **14** 33
[8] Gilbert M R and Sublet J Ch 2011 *Nucl. Fusion* **51** 043005
[9] Barnes R S 1965 *Nature* **206** 1307
[10] Ullmaier H 1984 *Nucl. Fusion* **24** 1039
[11] Lejcek P and Hofmann S 1995 *Crit. Rev. Sol. State Mater. Sci.* **20** 1
[12] Briant C L and Messmer R P 1982 *J. Phys.* **43** 255
[13] Satou M, Koide H, Hasegawa A, Abe K, Kayano H and Matsui H 1996 *J. Nucl. Mater.* **233** 447
[14] Fedorov A V, van Veen A and Ryazanov A I 1996 *J. Nucl. Mater.* **233** 385
[15] Fedorov A V, Buitenhuis G P, Veen A V, Ryazanov A I, Evans J H, Witzenburg W V and Westerduin K T 1996 *J. Nucl. Mater.* **227** 312
[16] Ryazanov A I, Manichev V M and W V Witzenburg 1996 *J. Nucl. Mater.* **227** 304
[17] Ryazanov A I, Matsui H and Kazaryan A V 1999 *J. Nucl. Mater.* **271** 356
[18] Hoelzer D T and Rowcliffe A F 2000 *Proceedings of 5th IEA and JUPITER Joint Workshop on Vanadium Alloys for Fusion Applications*, Tokyo, p. 43
[19] Valiev R Z, Khairullin V G and Sheikh-Ali A D 1991 *Structure and Property Relationships for Interfaces*, edited by Walter J L, King A H and Tangri K (ASM International, Metals Park, OH), p. 309
[20] Martin G 1998 *Curr. Opin. Solid State Mater. Sci.* **3** 552
[21] Zinkle S J and Singh B N 2000 *J. Nucl. Mater.* **283** 306
[22] Hampel K, Vvedensky D D and Crampin S 1993 *Phys. Rev. B* **47** 4810
[23] Campañá C, Boyle K P and Miller R E 2008 *Phys. Rev. B* **78** 134114
[24] Zhang L, Zhang Y, Geng W T and Lu G H 2012 *Europhys. Lett.* **98** 17001
[25] Campbell G H, Belak J and Moriarty J A 1999 *Acta Mater.* **47** 3977
[26] Janisch R and Elsässer C 2003 *Phys. Rev. B* **67** 224101
[27] Janisch R and Elsässer C 2008 *Phys. Rev. B* **77** 094118
[28] Campbell G H, Foiles S M, Gumbsch P, Rühle M and King W E 1993 *Phys. Rev. Lett.* **70** 449
[29] Perdew J P, Burke K and Ernzerhof M 1996 *Phys. Rev. Lett.* **77** 3865
[30] Kresse G and Hafner J 1993 *Phys. Rev. B* **47** 558
[31] Kresse G and Furthmüller J 1996 *Phys. Rev. B* **54** 11169
[32] Kresse G and Furthmüller J 1996 *Comput. Mater. Sci.* **6** 15
[33] Bolef D I, Smith R E and Miller J G 1971 *Phys. Rev. B* **3** 4100
[34] Monkhorst H J and Pack J D 1976 *Phys. Rev. B* **13** 5188
[35] Zhou H B, Jin S, Shu X L, Zhang Y, Lu G H and Liu F 2011 *Europhys. Lett.* **96** 66001
[36] Zhang P B, Zhao J J, Qin Y and Wen B 2011 *J. Nucl. Mater.* **419** 1
[37] Puska M J, Nieminen R M and Manninen M 1981 *Phys. Rev. B* **24** 3037
[38] Zhang S J, Kontsevoi O Y, Freeman A J and Olson G B 2011 *Acta Mater.* **59** 6155
[39] Tian Z X, Yan J X, Hao W and Xiao W 2011 *J. Phys.: Condens. Matter* **23** 015501
[40] Lu G and Kioussis N 2001 *Phys. Rev. B* **64** 024101
[41] Lu G H, Deng S, Wang T, Kohyama M and Yamamoto R 2004 *Phys. Rev. B* **69** 134106
[42] Chen Z Z and Wang C Y 2006 *Chin. Phys.* **15** 604
[43] Wang Y B, Zhang G, Liu M J, Chen X L and Chen J 2009 *Chin. Phys. B* **18** 1181
[44] Rice J R 1992 *J. Mech. Phys. Solids* **40** 239
[45] Fu C L 1990 *J. Mater. Res.* **5** 971
[46] Rice J R and Thomson R 1974 *Philos. Mag.* **29** 73
[47] Gong H R 2009 *Intermetallics* **17** 562
[48] Lu G, Orlikowski D, Park I, Politano O and Kaxiras E 2002 *Phys. Rev. B* **65** 064102
[49] Yuasa M, Nishihara D, Mabuchi M and Chino Y 2012 *J. Phys.: Condens. Matter* **24** 085701
[50] Zhang Q, Fan T W, Fu L, Tang B Y, Peng L M and Ding W J 2012 *Intermetallics* **29** 21
[51] Rice J R, Beltz G E and Sun Y 1992 *Topics in Fracture and Fatigue*, edited by Argon A S (Berlin: Springer)